Chitosan Modified with a Polydentate Crosslinker for Metal-Ion Adsorption

K. R. Krishnapriya, M. Kandaswamy

Department of Inorganic Chemistry, University of Madras, Chennai, India

Received 30 January 2009; accepted 7 May 2009
DOI 10.1002/app.30840
Published online 30 October 2009 in Wiley InterScience (www.interscience.wiley.com).

ABSTRACT: The chemical modification on chitosan (CTS) was carried out by cross-linking it with precursor compound 3,3′-dimethoxy-4,4′-dihydroxy-5,5′-bis(N,N′-piperazine-1-yl methyl benzaldehyde), (PC) in order to improve the metal ion adsorption capacities and selectivity of the product. The resulting crosslinked chitosan derivative (CCTSL) was characterized by elemental analysis, Fourier transform infrared spectrum (FTIR), Differential Scanning calorimetry (DSC), Scanning Electron Microscopy (SEM) and powder X-ray diffraction (XRD) studies. Adsorption experiments (pH dependency, kinetics, and equilibrium) of CCTSL towards various metal ions (Mn^{2+}, Fe^{2+}, Co^{2+}, Cu^{2+}, Ni^{2+}, Cd^{2+} and Pb^{2+}) were investigated. The adsorption was dependent on pH of the solution, with a maximum capacity between pH 6.5 and 8.5. The adsorption kinetics data were best fitted with pseudo second-order model, which gave a correlation coefficient of 0.999. The adsorption process could be described with Langmuir isotherm (R = 0.999), which revealed that the maximum capacity for monolayer saturation was 79 mg Cu(II) per gram of CCTSL (1.24 mmol g^{-1}). From the studies, we also infer that the order of metal adsorption capacities in mmol g^{-1} for the derivative is $Cu^{2+} > Ni^{2+} > Co^{2+} \geq Fe^{2+} \geq Cd^{2+} \geq Mn^{2+} \geq Pb^{2+}$. Hence this material can be used to extract Cu^{2+} ions from industrial effluents. © 2009 Wiley Periodicals, Inc. J Appl Polym Sci 115: 3013–3023, 2010

Key words: adsorption; biopolymers; metal–polymer complexes; synthesis; transition metal chemistry

INTRODUCTION

Natural polysaccharide chitosan and its derivatives have great potential applications in the areas of biotechnology, biomedicine, food ingredients, and cosmetics because of their many useful features, such as hydrophilicity, biocompatibility, biodegradability, antibacterial properties, and remarkable affinity for many biomacromolecules.[1–6] Also, because the amino groups can serve as chelation sites, chitosan and its derivatives are capable of adsorbing a number of metal cations and can be used as adsorbent material for the removal of metal cations from wastewater or effluents.[7–10] The modification of the polymer surface through the introduction of new complexation groups may result in the formation of efficient chelates, which thus increases its adsorption capacity and selectivity toward metal ions in solution.[11–13] Generally, various studies have been conducted to make derivatives of chitosan by chemical modification techniques, such as grafting, sulfonation, quaternization, hydroxylation, and carboxymethylation. Among the derivatives, the grafting of carboxylic functions has been regarded frequently as an interesting process for increasing the adsorption properties of chitosan.

In this study, a new crosslinked chitosan derivative (CCTSL) was prepared by the reaction of chitosan with a newly reported compound, 3,3′-dimethoxy-4,4′-dihydroxy-5,5′-bis(*N*,*N*′-piperazine-1-yl methyl benzaldehyde) (a crosslinker), in a suitable solvent. The purpose of this modification was to design a chelating derivative for the extraction of metal ions from aqueous solution (industrial effluents) via coordination. To evaluate the adsorbent capacity of the new polymer, various metal ions, including Mn^{2+}, Fe^{2+}, Co^{2+}, Cu^{2+}, Ni^{2+}, Cd^{2+}, and Pb^{2+}, were used.

EXPERIMENTAL

Materials

Chitosan of (Sigma-Aldrich Chemicals Pvt. Ltd., Bangalore, India) low molecular weight was purchased from Aldrich (catalog no. 44,8869) with a deacetylation percentage in the range 75–85% and used as received. We prepared stock solutions (1000 mg/L) of Mn^{2+}, Fe^{2+}, Co^{2+}, Cu^{2+}, and Ni^{2+} by dissolving the appropriate amount of metal(II) sulfate (analytical grade) in double-distilled water and

Correspondence to: M. Kandaswamy (mkands@yahoo.com).

Contract grant sponsor: Indian Department of Science and Technology (through Department of Science and Technology/Science and Engineering Research Council project SR/S1/IC-27/2004 to K.R.K.).

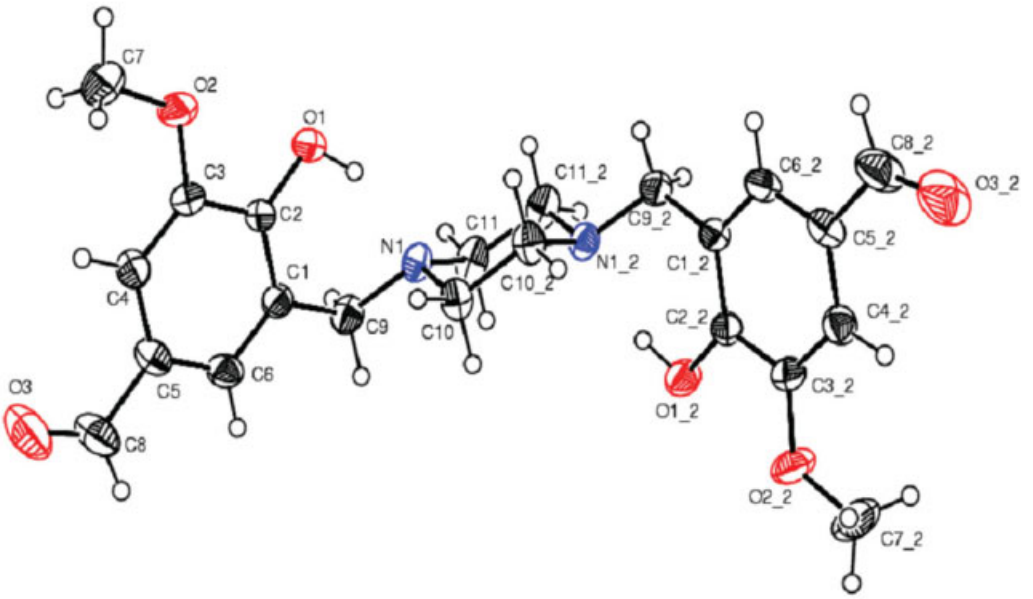

Figure 1 Oak Ridge thermal ellipsoid plot diagram of the crosslinker. [Color figure can be viewed in the online issue, which is available at www.interscience.wiley.com.]

standardized them with a standard solution of 0.01 mol/L ethylene diamine tetraacetic acid.[14] We also prepared stock solutions (1000 mg/L) of Cd^{2+} and Pb^{2+} by dissolving the appropriate amount of their metal (II) nitrates (analytical grade) in double-distilled water. Working standard solutions of all of the metal ions were prepared through the dilution of the respective 1000-mg/L stock solution with distilled water. All other chemicals and solvents were analytical grade and were used as received.

Synthesis of a new crosslinker: 3,3′-Dimethoxy-4,4′-dihydroxy-5,5′-bis(*N*,*N*′-piperazine-1-yl methyl benzaldehyde)

A mixture of piperazine (4.3 g, 0.05 mol) and paraformaldehyde (3.2 g, 0.1 mol) and 3-methoxy-4-hydroxybenzaldehyde (15.2 g, 0.1 mol) in a 40 : 10 (v/v) mixture of ethanol (EtOH) and acetic acid (AcOH; 200 mL) was stirred for 6 h at 50°C. It was then cooled to room temperature and neutralized with solid Na_2CO_3 (9.25 g). EtOH was removed by distillation under reduced pressure, and the residue was extracted with chloroform. The removal of chloroform by distillation yielded a white crystalline solid, which was further purified by silica gel column chromatography with chloroform–light petroleum (bp = 60–80°C, 3 : 7 v/v) as the eluent. The pure compound was obtained as white crystals suitable for X-ray diffraction (XRD) analysis, which were obtained by the slow evaporation of the eluted solvent.

Yield = 15 g (72%). mp = 232°C. ANAL. Calcd for $C_{22}H_{26}N_2O_6$: C, 63.76%; H, 6.32%; N, 6.76%. Found: C, 63.65%; H, 6.39%; N, 6.72%. Mass (electron impact) m/z: 414 (M^+). Selected Fourier transform

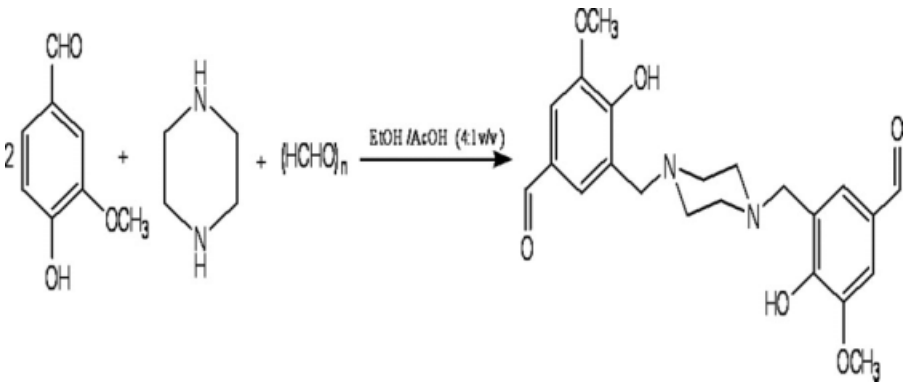

Scheme 1 Synthesis of the precursor compound 3,3′-dimethoxy-4,4′-dihydroxy-5,5′-bis(*N*,*N*′-piperazine-1-yl methyl benzaldehyde).

TABLE I
Crystal Data and Structure Refinement for the Crosslinker

Empirical formula	$C_{22}H_{26}N_2O_6$
CCDC number	673666
Formula weight	414.45
Temperature	293(2) K
Wavelength	0.71073 Å
Crystal system	Monoclinic
Space group	C2/c
Unit cell dimensions	$a = 20.2347(5)$ Å; $\alpha = 90.00°$ $b = 9.5071(3)$ Å; $\beta = 125.9690(10)°$ $c = 13.6286(4)$ Å; $\gamma = 90.00°$
Volume	2121.90(11) Å^3
Z	4
Density (calculated)	1.297 mg/m^3
Absorption coefficient	0.095 mm^{-1}
$F(000)$	880
Crystal size	0.30 × 0.20 × 0.18 mm^3
Index ranges	$-11 \leq h \leq 11$; $-13 \leq k \leq 9$; $-14 \leq l \leq 14$
Reflections collected	7400
Independent reflections	2298 [R(int) = 0.1164]
Completeness to 2θ	99.3%
Refinement method	Full-matrix least squares on F^2
Data/restraints/parameters	2298/0/195
Goodness of fit on F^2	0.93
Final R indices [$I > 2\sigma(I)$]	$R_1 = 0.062$, $wR_2 = 0.146$
R indices (all data)	$R_1 = 0.097$, $wR_2 = 0.172$
Largest difference peak and holes	0.33 and −0.32 e/Å^3

TABLE II
Selected Bond Lengths of the Crosslinker

C1 C6	1.3850(16)
C1 C2	1.3954(14)
C1 C9	1.5033(16)
C2 O1	1.3509(13)
C2 C3	1.4038(16)
C3 O2	1.3601(17)
C3 C4	1.3974(17)
C4 C5	1.3974
C4 H4	0.9300
C5 C6	1.3788(18)
C5 C8	1.4660918)
C6 H6	0.9300
C7 O2	1.4112(17)
C7 H7A	0.9600
C7 H7B	0.9600
C7 H7C	0.9600
C8 O3	1.199(2)
C8 H8	0.963(18)
C9 N1	1.4722(16)
C9 H9A	0.9700
C9 H9B	0.9700
C10 N1	1.4643(15)
C10 C10	1.501(2) 2_655
C10 H10A	1.013(15)
C10 H10B	0.966(15)
C11 N1	1.4616(15)
C11 C11	1.510(3) 2_655
C11 H11A	0.993(16)
C11 H11B	0.992(17)
O1 H1	0.910(19)

infrared (FTIR) data (KBr, ν, cm^{-1}): 1626, 1558, 3447. ^{1}H-NMR ($CDCl_3$, δ, ppm): 2.56 (bs, N—**CH_2**—**CH_2**—N, 8H), 3.84 (s, Ar—**CH_2**—N, 4H), 3.94 (s, **CH_3**O, 6H), 7.18 (s, **Ar—H**, 2H), 7.36 (s, **Ar—H**, 2H), 9.78 (s, CHO, 2H). ^{13}C-NMR ($CDCl_3$, δ, ppm): 52.1 (NCH_2); 56.0 (OCH_3); 60.4 (N—CH_2—Ar); 109.7, 120.3, 125.5, 128.5, 148.6–153.2 (ArC); 190.5 (CHO). Single-crystal analysis Cambridge Crystallographic Data Centre (CCDC) no. 196207.

Synthesis of CCTSL

We prepared CCTSL by dissolving 1.0 g of chitosan powder (0.0048 mol of glucosamine residue) in 25 mL of 1 wt % AcOH, diluted with methanol

TABLE III
Selected Bond Angles of the Crosslinker

C6 C1 C2	118.63(110)
C6 C1 C9	121.02(10)
C2 C1 C9	120.24(10)
O1 C2 C1	121.80(10)
O1 C2 C3	117.85(9)
C1 C2 C3	120.34(10)
O2 C3 C4	125.34(10)
O2 C3 C2	114.28(10)
C4 C3 C2	120.19(10)
C3 C4 C5	119.47(11)
C3 C4 H4	120.3
C5 C4 H4	120.3
C6 C5 C4	120.36(11)
C6 C5 C8	118.88(12)
C4 C5 C8	120.76(13)
C5 C6 C1	120.93(10)
C5 C6 H6	119.5
C1 C6 H6	119.5
O2 C7 H7A	109.5
O2 C7 H7B	109.5
H7A C7 H7B	109.5
O2 C7 H7C	109.5
H7A C7 H7C	109.5
H7B C7 H7C	109.5
O3 C8 C5	125.79(15)
O3 C8 H8	122.39110
C5 C8 H8	111.9(11)
N1 C9 C1	112.68(9)
N1 C9 H9A	109.1
C1 C9 H9A	109.1
N1 C9 H9B	109.1
C1 C9 H9B	109.1
H9A C9 H9B	107.8
N1 C10 C10	110.40(9) 2_655
N1 C10 H10A	110.7(9)
C10 C10 H10A	110.9(8) 2_655
N1 C10 H10B	107.8(9)
C10 C10 H10B	109.8(9) 2_655
H10A C10 H10B	107.1912)
N1 C11 C11	110.77(10) 2_655
N1 C11 H11A	107.3(9)
C11 C11 H11A	111.1(9) 2_655
N1 C11 H11B	107.3(10)
C11 C11 H11B	108.8(10) 2_655
H11A C11 H11B	111.5(13)
C11 N1 C10	109.58(9)

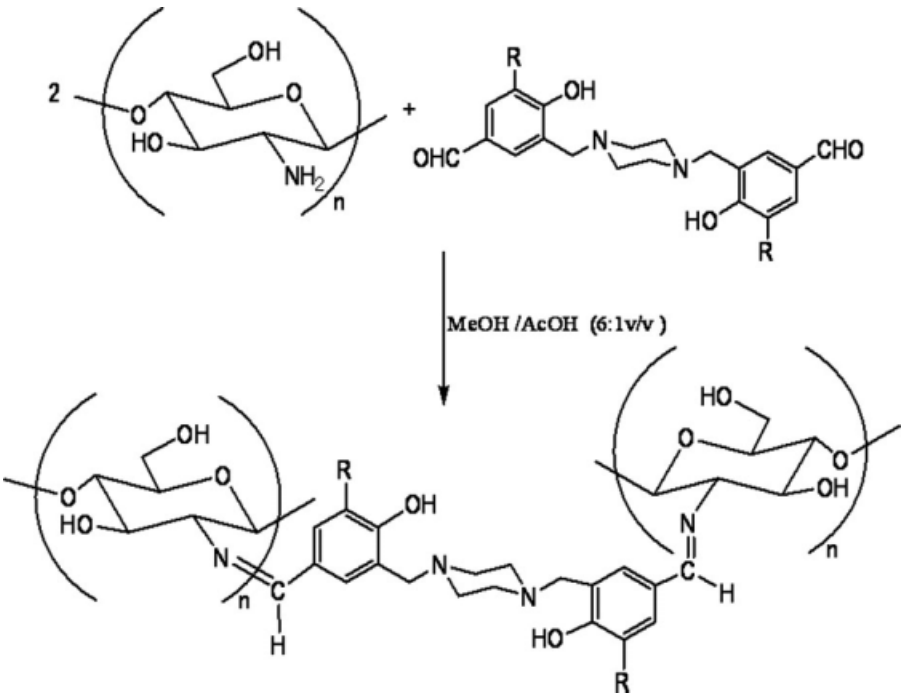

Scheme 2 Synthesis of the CCTSL.

(MeOH; 150 mL) and then treating it with 1.0 g of 3,3′-dimethoxy-4,4′-dihydroxy-5,5′-bis(*N,N*′-piperazine-1-yl methyl benzaldehyde) (0.0024 mol) dissolved in chloroform (20 mL). The mixture was stirred at room temperature for 16 h; it was then refluxed for 18 h, which resulted in a brown gel. It was then decanted and thoroughly washed with chloroform to remove any unreacted crosslinker and then dried *in vacuo* at 60°C to give CCTSL as a white powder.

Yield = 1.7 g (85%). ANAL. found for CCTSL: C, 54.23%; H, 59.6%; N, 5.25%.

Preparation of metal–CCTSL

The metal complexes of CCTSL were prepared by the addition of 50.0 mL of 100-mg/L metal-ion (Mn^{2+}, Fe^{2+}, Co^{2+}, Cu^{2+}, Ni^{2+}, Cd^{2+}, and Pb^{2+}) solutions buffered at pH 7.5 and were placed in contact with 50 mg sample of crosslinked chitosan (CCTSL) for a period of 4 h by agitation. After 4 h, the shaking was turned off, and immediately thereafter, the adsorbent material was decanted and dried at 60°C.

Instrumentation

Elemental analysis was carried out on a Carlo Erba model 1106 elemental analyzer (Milano, Italy). FTIR spectra were recorded on a PerkinElmer RX1 model spectrophotometer (Amsterdam, Netherlands) on KBr discs in the wave-number range 4000–250 cm^{-1}. ^{1}H-NMR and ^{13}C-NMR spectra were recorded with a model FX-80-Q Fourier transform nuclear magnetic resonance spectrometer (Peabody, USA). Differential scanning calorimetry (DSC) analysis was carried out with a Shimadzu DSC-50 (Schimadzu Scientific Instruments, USA), and the scanning was carried out within the temperature range 25–800°C at a heating rate of 10°C/min under a nitrogen atmosphere. Powder XRD studies were carried out with a scientific high-resolution Guinier X-ray powder diffractometer with Cu $K\alpha_1$ radiation with a quartz monochromator (Ahrensburg, Germany). Micrographs of CCTSL before and after metal(II) ion adsorption were taken with a JEOL JSM-5600LV scanning electron microscope (Shelton, USA). The metal(II) ion concentration was measured with a

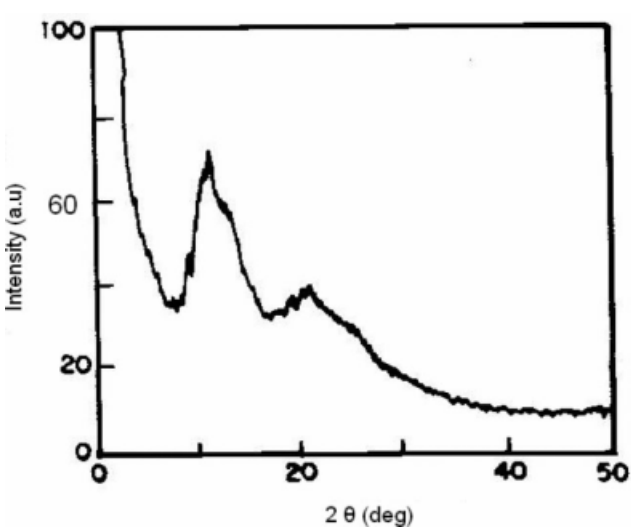

Figure 2 Powder XRD patterns of CCTSL.

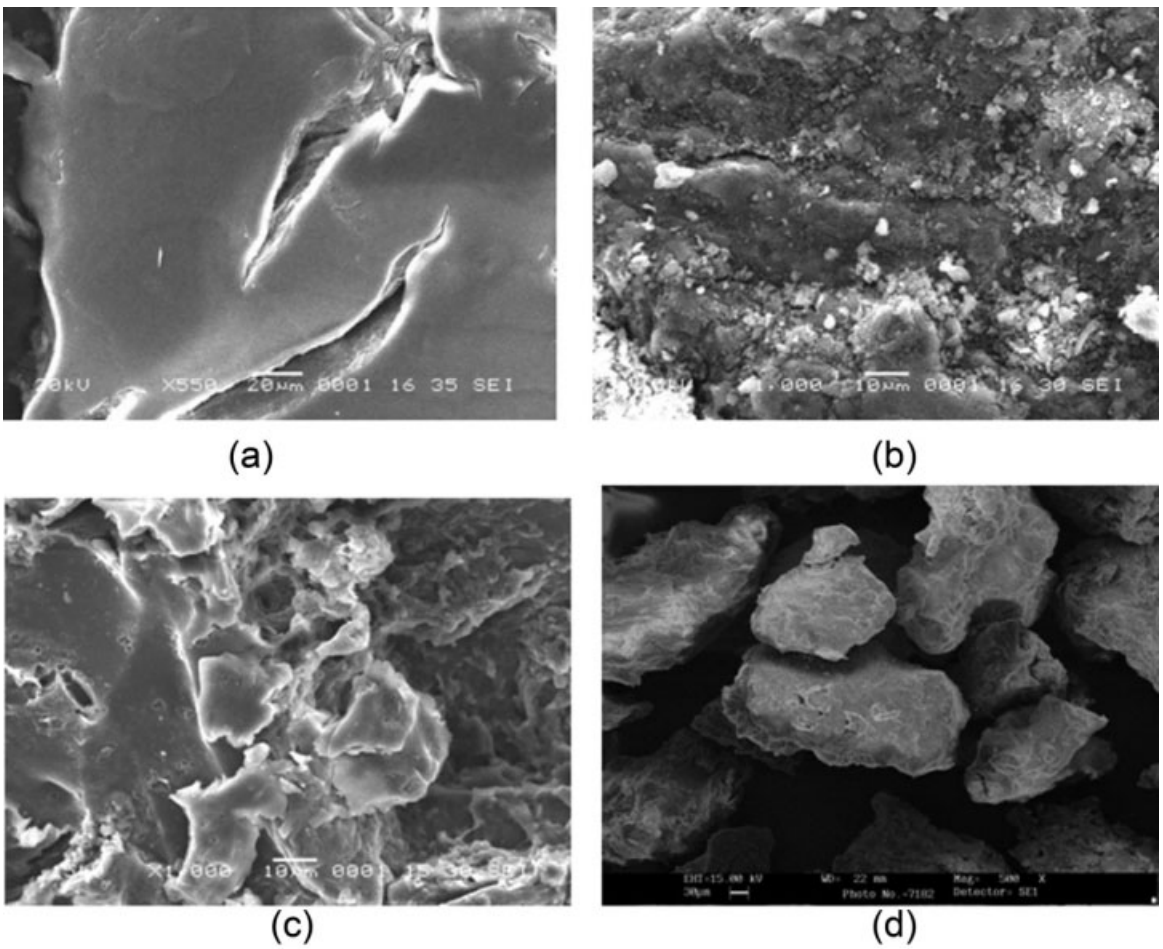

Figure 3 SEM images of (a) chitosan, (b) CCTSL, (c) Cu–CCTSL, and (d) Fe–CCTSL.

PerkinElmer AAnalyst 750 atomic absorption spectrophotometer. The molecular structure of the crosslinker 3,3′-dimethoxy-4,4′-dihydroxy-5,5′-bis(*N*,*N*′-piperazine-1-yl methyl benzaldehyde) was solved by a single-crystal XRD method. The crystal data were collected on a Bruker Smart Apex charged coupling device diffractometer equipped with a fine-focus sealed tube that used graphite monochromatized Mo Kα radiation with an ω scan mode and refined by full-matrix least-squares procedures. SHELXS97 and SHELXL97 programs[15] were used for structure solution and structure refinement, respectively. The Oak Ridge thermal ellipsoid plot diagram of crosslinker is shown in Figure 1 (CCDC no. 673666).

Adsorption experiments

Effect of the pH on the adsorption

The adsorption properties of CCTSL and the effect of the pH on adsorption were carried out from pH 3 to 10 with various buffer solutions [KCl/HCl for pH = 2 and 3; AcOH/sodium acetate for pH = 4, 5, and 6; tris(hydroxymethyl) aminomethane/HCl for pH = 7.5 and 8.5; and ammonia/ammonium chloride for pH = 9.5 and 10]. Aliquots (50.0 mL) of 100 mg/L of metal-ion solutions buffered at different pH values were placed in contact with 50-mg samples of modified chitosan (CCTSL) for a period of 2 h by agitation. After 4 h, the shaking was turned off. Immediately thereafter, the adsorbent material was decanted, and 2 mL of the filtrate was removed and diluted in volumetric flasks to determine the metal-ion concentration by atomic absorption spectrophotometry. Each run was duplicated under identical conditions. The quantity of metal(II) ions adsorbed at different pH values was calculated as follows:[16–19]

$$Q_e = \frac{(C_0 - C_e)V}{W}, \quad (1)$$

where Q_e is the equilibrium adsorption capacity of CCTSL (mg/g of adsorbent); V is the volume of solution (mL); C_0 and C_e are the initial and equilibrium concentrations of the solute, respectively; and W is the weight of the sorbent (g).

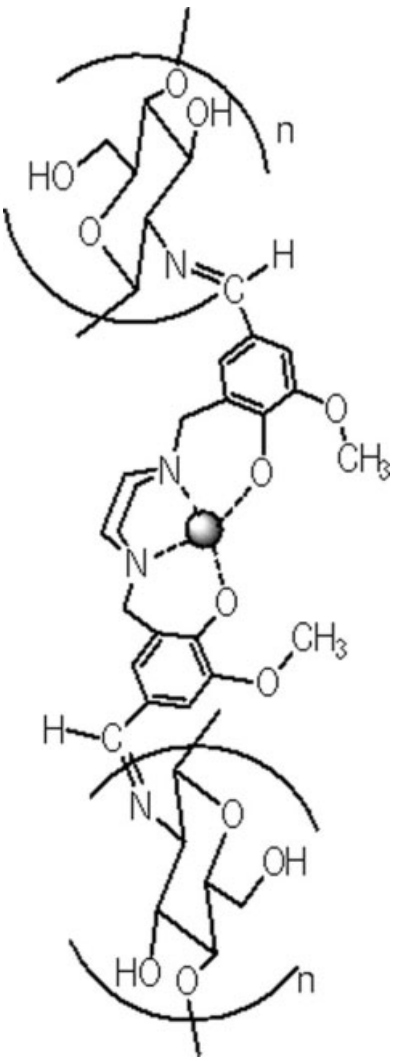

Figure 4 Metal–CCTSL.

The amount of metal ions adsorbed by the adsorbent can also be calculated as follows:

$$q_e = \frac{(C_0 - C_e)V}{WM}, \quad (2)$$

where q_e is the adsorption capacity of the adsorbent at equilibrium (mmol of metal ion/g of adsorbent) and M is the atomic weight of the corresponding metal ion.

Adsorption kinetics

The adsorption kinetics of CCTSL toward Cu(II) ions was determined at pH 8.5. CCTSL (50 mg) and Cu(II) ion solution (50.0 mL) buffered at 8.5 were shaken with an orbital shaker (Rivotek, Chennai, India) at 200 rpm for 2 h. After predetermined time periods, 2-mL aliquots were removed, and the concentrations of Cu(II) ions in the solutions were measured.

Adsorption equilibrium isotherms

Samples of CCTSL (50.0 mg) were added to 25.0 mL of Cu(II) ion solution at several concentrations and previously buffered to the optimum adsorption pH. After this procedure, they were kept under stirring until the adsorption equilibrium was reached. Aliquots were taken and diluted to determine the metal-ion concentration by atomic absorption spectrophotometry. The adsorption process was fast, reached equilibrium after 2 h, and remained constant for 24 h.

RESULTS AND DISCUSSION

Synthesis and characterization of the crosslinker

The crosslinker was prepared by the Mannich base reaction of piperazine with 3-methoxy-4-hydroxybenzaldehyde in the presence of paraformaldehyde, as shown in Scheme 1. It was characterized by FTIR and NMR spectral techniques. NMR was consistent with the proposed structure. The FTIR spectra of this compound exhibited a band at 3447 cm^{-1} due to υ(—OH) stretching. The peak around 1626 cm^{-1} was due to the presence of υ(C=O) of the aldehyde group present in the compound. The peak at 1558 cm^{-1} appeared because of the presence of υ(C=C) stretching of the aromatic group.[20] The ^{1}H-NMR spectra of the compound exhibited a singlet peak

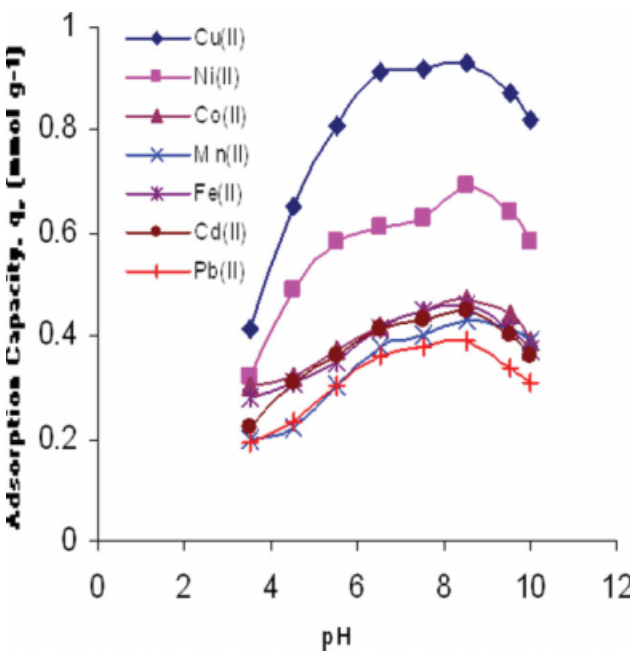

Figure 5 Effect of pH on metal(II)-ion adsorption by CCTSL ([M^{2+}] = 100 mg/L; temperature = 25°C; contact time = 2 h; shaking rate = 200 rpm; adsorbent mass = 50 mg). [Color figure can be viewed in the online issue, which is available at www.interscience.wiley.com.]

TABLE IV
Concentrations of the Metal Ions Before and After Treatment with the Adsorbent at pH 6.5

Metal(II) ion	Cu(II)	Ni(II)	Co(II)	Mn(II)	Fe(II)	Cd(II)	Pb(II)
Initial concentration (ppm)	99.8	99.6	99.5	99.8	99.7	99.3	99.4
Residual concentration (ppm)	40.9	59.1	71.8	76.2	74.3	49.5	29.7

around at 9.78 ppm because of the presence of aldehyde protons. The appearance of peaks around 7.18–7.36 ppm indicated the presence of aromatic protons. The singlets appearing in the region at 3.84 ppm were due to benzylic protons, and the peak at 3.94 ppm was due to methoxy and benzylic protons. A broad singlet was obtained around 2.56 ppm for piperazine N—CH_2 protons of the compound. The ^{13}C-NMR spectra of the compound showed peaks at 52.1, 56.0, 60.4, 109.0–154.0, and 190.5 ppm, which indicated the presence of N—CH_2, OCH_3, Ar—CH_2, aromatic(C), and CHO carbons, respectively.[20]

XRD studies

The molecular formula of the crosslinker, 3,3′-dimethoxy-4,4′-dihydroxy-5,5′-bis(*N*,*N*′-piperazine-1-yl methyl benzaldehyde), was $C_{22}H_{26}N_2O_6$. The compound crystallized in the monoclinic space group C2/c with one molecule in the unit cell. The dimensions of the unit cell were a = 20.2347(5) Å, b = 9.5071(3) Å, c = 13.6286(4) Å, β = 125.9690(10)°, Z = 4. The piperazine ring in the ligand adopted a chair conformation, as shown in Figure 1. The crystal data of the crosslinker and its selected bond lengths and bond angles are given in Tables I–III, respectively.

Synthesis and characterization of CCTSL

The new CCTSL was obtained by the crosslinking of 2 equiv of chitosan with 1 equiv of crosslinker. The reaction between aldehyde groups from the crosslinker and amine groups from chitosan provided Schiff base formation, which led to crosslinking in the polymeric structure, as shown in Scheme 2. The crosslinking precursor compound introduced coordinating groups into the chitosan, such as phenolic, amine, and piperazine moieties, which conferred metal-ion chelation properties to the new adsorbent. Hence, this new adsorbent had a special characteristic, in that it did not require the use of additional crosslinking agents, such as glutaraldehyde, whereas the crosslinker acted as a crosslinking agent and a coordinating agent.

The new adsorbent material was characterized by spectral, thermal, and powder XRD studies. The surface modification of the material was analyzed with scanning electron microscopy (SEM).

Elemental analysis showed the C/N ratios to be 6.05 and 10.33 for chitosan and CCTSL, respectively. From this, we inferred that the functional group attached to the chitosan was around 66%. The IR spectra of CCTSL exhibited an additional peak around 3420 cm^{-1} for the phenolic —OH group apart from a strong peak at 3440–3446 cm^{-1} for chitosan (CTS), which corresponded to the stretching vibration of the —N—H and —OH groups. There were two absorption bands observed around 1610–1650 cm^{-1}. The additional band in this region was due to the presence of an imine (—C=N) group in this derivative. The band at 1067 cm^{-1} assigned to the stretching vibration of a secondary >C—OH group shifted toward a lower wavelength (1020–1010 cm^{-1}), which may have been due to a steric effect that resulted from the condensation of the crosslinker to CTS. Furthermore, the peaks around 1400–1500 cm^{-1} were due to aromatic backbone vibration, and the peak around 1250–1265 cm^{-1} was due to the phenolic C—O group of the crosslinker moiety.[21–24]

The DSC thermogram for CCTSL exhibited an endothermic peak in the region 60–100°C and an exothermic peak in the region 320–360°C. It is well known that, for chitosan and its derivatives, endothermic peaks are observed for water vapor elimination in the polymer matrix and exothermic peaks are observed for the decomposition of the polymer.[21] There were some differences with respect to the endothermic and exothermic peaks of chitosan and its derivatives, which may have been the result of chemical modification carried on chitosan.

Powder XRD patterns of CCTSL are shown in Figure 2 and are compared with that of CTS.[21] CTS

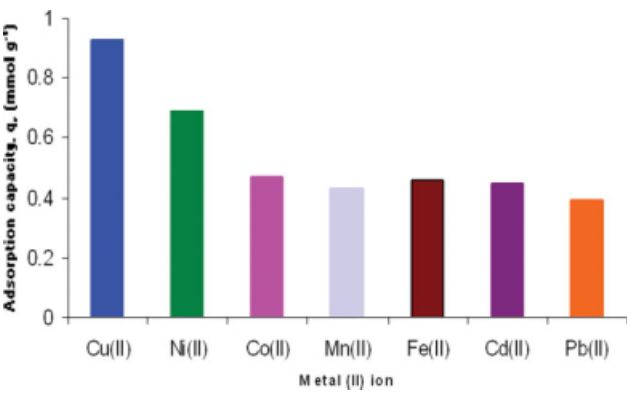

Figure 6 Adsorption capacities of CCTSL [i.e., q_e (mmol/g)] at pH 8.5. [Color figure can be viewed in the online issue, which is available at www.interscience.wiley.com.]

TABLE V
Adsorption Capacities of CCTSL at pH 6.5

Metal(II) ion	Cu(II)	Ni(II)	Co(II)	Mn(II)	Fe(II)	Cd(II)	Pb(II)
Q_e (mg/g)	59.09	40.5	27.7	23.62	25.69	50.58	70.81
q_e (mmol/g)	0.93	0.69	0.47	0.43	0.46	0.45	0.34

shows the characteristic peak at 2θ = 10°C due to the presence of (001) and (100) and that at 2θ = 20°C caused by the presence of (101) and (002). For CCTSL, the intensity of peaks at 2θ = 10 and 20°C decreased, and the peaks were broadened more than that of CTS. We believe that the decrease in the crystallinity of the chitosan derivative could have been due to a deformation of the strong hydrogen bond in the free chitosan molecule and also to the bulkier compound (crosslinker) substitution onto it. This low crystallinity indicated that they were considerably more amorphous than free chitosan.

The difference in structural morphology between the CTS and CCTSL copolymer was also further supported by the difference in their SEM images (Fig. 3). A micrograph of CCTSL displayed a more extensive three-dimensional network compared with the smooth lacunose surface of CTS,[25] which was attributed to the immobilization of a crosslinker on the polymer surface.

Preparation and characterization of metal–CCTSL

The metal complexes of CCTSL were prepared by the adsorption of 1 mol of metal(II) ions, such as Mn^{2+}, Fe^{2+}, Co^{2+}, Cu^{2+}, Ni^{2+}, Cd^{2+}, and Pb^{2+} ions, on the equimolar chitosan derivative (glucosamine unit) in aqueous solution (pH = 7.5). The proposed structure for the metal-complexed CCTSL is shown in Figure 4. The resulting metal–CCTSL was characterized with FTIR spectral analysis and SEM analysis. The FTIR spectra of Cu–CCTSL when examined showed adsorption bands at 514 and 462 cm^{-1} due to the stretching vibrations of N—Cu and O—Cu, respectively. Furthermore, new bands near 600–500 cm^{-1} indicated the presence of SO_4^{2-} ions in the resulting Cu–CCTSL complex.

When the SEM images of Cu–CCTSL and Fe–CCTSL (Fig. 3) were compared to that of CTS and CCTSL, the surface of the metal-complexed derivatives exhibited more pores, which may have been due to the metal sites coordinated to the chitosan derivative.[26,27]

Adsorption studies

Effect of the pH on the adsorption

The effect of pH on the adsorption of the metal ions Mn^{2+}, Fe^{2+}, Co^{2+}, Cu^{2+}, Ni^{2+}, Cd^{2+}, and Pb^{2+} by CCTSL is illustrated in Figure 5. From this study, we inferred that the adsorption capacity of the modified chitosan derivative was affected by the pH.[16–19] The metal(II) ion adsorption by CCTSL increased with the pH of the solution from 3.5 to a maximum value of 6.5–8.5 and then decreased when the pH

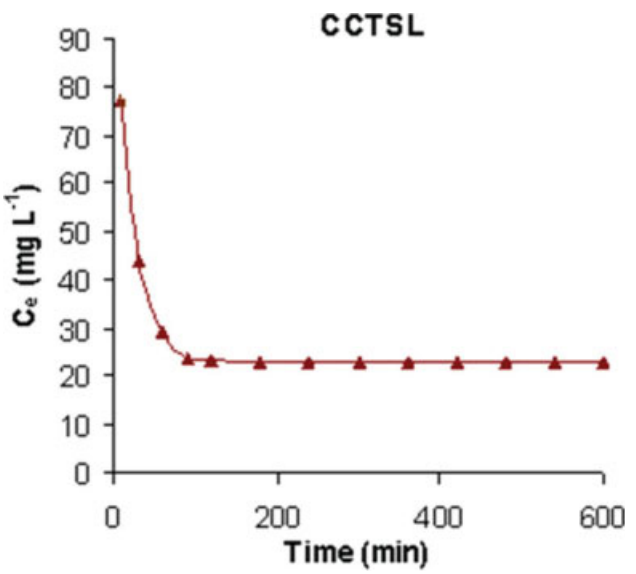

Figure 7 Kinetics of adsorption of Cu^{2+} ions by CCTSL ([M^{2+}] = 100 mg/L; pH = 8.5; temperature = 25°C; contact time = 2 h; shaking rate = 200 rpm; adsorbent mass = 50 mg). [Color figure can be viewed in the online issue, which is available at www.interscience.wiley.com.]

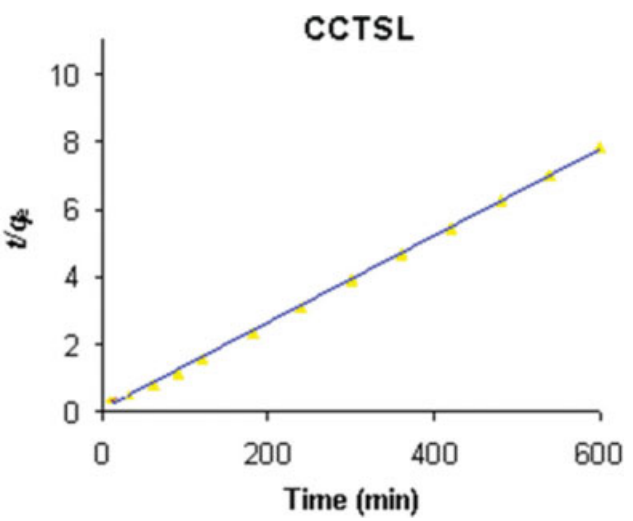

Figure 8 Linearization plot for the kinetics of adsorption of Cu^{2+} ions by CCTSL. [Color figure can be viewed in the online issue, which is available at www.interscience.wiley.com.]

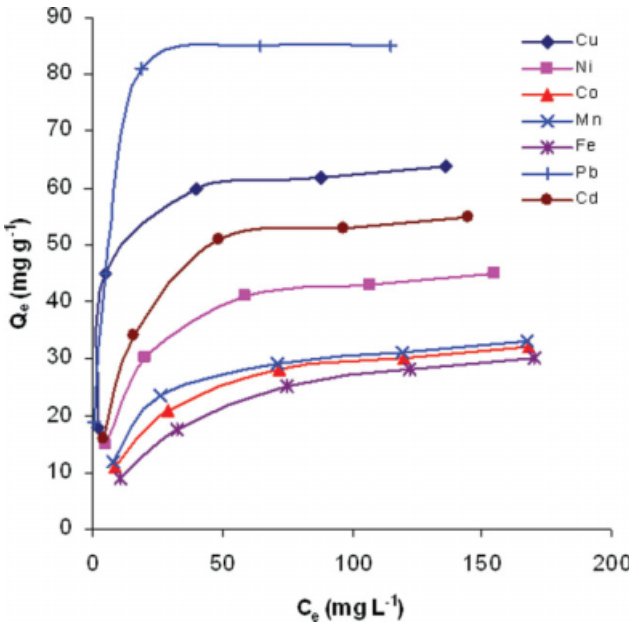

Figure 9 Adsorption equilibrium isotherms by CCTSL (temperature = 25°C; contact time = 1 h; adsorbent mass = 50 mg). [Color figure can be viewed in the online issue, which is available at www.interscience.wiley.com.]

increased beyond 8.5. At acidic pH 3.5 to 5.5, the lower adsorption of metal ions was attributed to the protonation of the complexation site (amine), which decreased the complex formation by the CCTSL with metal ions.[28,29] Around pH 6.5 to 8.5, the amino group existed as a free amine (without protonation), and in addition, the deprotonation took place at phenolic groups present in the chitosan derivative, which increased the metal-ion uptake by the adsorbent. At pH values above 8.5, the auxiliary complexation agents from buffer solutions formed complexes with the metal ion to avoid precipitation of metal hydroxide, which lowered the adsorption of the metal ion by the chitosan derivative. The results also indicate that CCTSL had a good adsorption capacity for Cu(II) ions in the pH ranges studied, which suggests possible selectivity for this metal ion. The adsorption capacities of CCTSL toward metal(II) ions studied in this work are given in Table IV and illustrated in Figure 6. The initial metal-ion concentration taken before adsorption was 100 ppm for all of the metal ions, and the residual concentrations of the filtrates in parts per million found from atomic absorption analysis are included in Table V.

These values were comparable to those of other chitosan derivatives reported in the literature.[30–33] From the studies, we inferred that the order of metal-ion adsorption capacities (mmol/g) for the derivative was $Cu^{2+} > Ni^{2+} > Co^{2+} \geq Fe^{2+} \geq Cd^{2+} \geq Mn^{2+} \geq Pb^{2+}$. CCTSL had a higher adsorption capacity toward Cu(II) ions than the other metal ions studied. This sequence maintained the trend of the well-known Irvin–Williams series.[34] The Cu(II) ions formed more stable complexes in aqueous solution with CCTSL than the other metal ions studied and, hence, showed maximum adsorption.

Adsorption kinetics

The kinetics of adsorption is one of the most important characteristics to be responsible for the efficiency of adsorption. Traditionally, the kinetics of interaction at a solid/solution interface is described by the expressions originally given by Lagergren, which are special cases for the general Langmuir rate equation.[35]

The fitting validity of these models is traditionally checked by the pseudo-first-order model, and the pseudo-second-order model was tested to interpret the experimental data. A good correlation of the kinetic data explained the adsorption mechanism of the metal ion on the solid phase.

The pseudo-first-order equation is represented as follows:

$$\log (Q_e - Q_t) = \log\ Q_e - \frac{k_1}{2.303} t \qquad (3)$$

where k_1 (min^{-1}) is the pseudo-first-order adsorption rate constant, Q_t (mg/g) is the amount adsorbed at time t (min), and Q_e (mg/g) denotes the amount adsorbed at equilibrium. The plots of log ($Q_e - Q_t$) versus t gave the k_1 and Q_e values.

The pseudo-second-order equation, which is based on the adsorption capacity at equilibrium, can be expressed by eq. (4):

$$\frac{t}{Q_t} = \frac{1}{k_2 Q_e^2} + \frac{1}{Q_e} t \qquad (4)$$

where k_2 (g mg^{-1} min^{-1}) is the adsorption rate constant of pseudo second order and Q_e can be obtained from the intercept and slope of the plot of (t/Q_t) versus t.

TABLE VI
Parameters for the Adsorption of Various Metal(II) Ions by CCTSL According to the Langmuir Isotherm Model

Metal(II) ion	Cu(II)	Ni(II)	Co(II)	Mn(II)	Fe(II)	Cd(II)	Pb(II)
K_L ($\times 10^{-2}$ L/mg)	25.5	8.8	4.9	6.4	3.0	6.5	30.6
Q_m (calcd; mg/g)	65.36	48.08	35.71	35.71	35.84	59.70	87.72

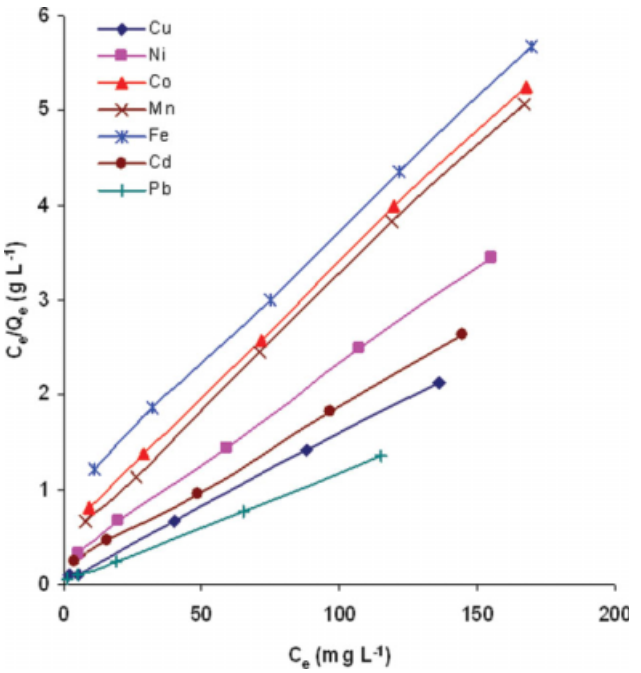

Figure 10 Linearization according to the Langmuir model of adsorption isotherms by CCTSL. [Color figure can be viewed in the online issue, which is available at www.interscience.wiley.com.]

The adsorption kinetics behavior of CCTSL toward Cu^{2+} ions is illustrated in Figure 7, and the linearization plot for the kinetics of the adsorption of Cu^{2+} ion by CCTSL is shown in Figure 8.

The kinetic curve for Cu(II) ions showed that the adsorption was rapid in the first few minutes, reached equilibrium after approximately 90 min, and remained constant for 24 h. The second-order rate constant obtained for CCTSL was 1.2×10^{-3} g mg^{-1} min^{-1}, and a Q_e (calcd) of 78.7 mg/g with a correlation coefficient (R) of 0.999 fit best when compared to a first-order rate constant of 3.2×10^{-2} min^{-1} and 37.6 mg/g with $R = 0.949$, where Q_e, experimentally found to be 77.1 mg/g, which showed that chemical sorption was the rate-limiting step of the adsorption mechanism and did not involve a mass transfer in solution.[36]

Adsorption isotherms

The equilibrium studies were carried out for CCTSL toward various metal(II) ions at the pH value of optimum adsorption (pH = 8.5) and with the necessary contact time to reach the adsorption equilibrium of each metal. The adsorption equilibrium isotherms for CCTSL were illustrated in Figure 9. In the figure, the relationship between the amounts of metal ion adsorbed on the adsorbent surface and the remaining metal-ion concentration in the aqueous phase at equilibrium can be observed. This relationship showed that the adsorption capacity increased with the equilibrium concentration of the metal ion in solution and progressively reached saturation of adsorbent. For interpretation of the adsorption data, the Langmuir isotherm model was used in this study. The following Langmuir equation took into account adsorption sites with the same energy, where the formation of a monolayer occurred on the surface of the adsorbent with saturation of the sites:

$$Q_e = \frac{K_L C_e Q_m}{1 + K_L C_e} \tag{5}$$

where Q_e and C_e were the amount adsorbed (mg/g) and the adsorbate concentration in solution (mg/L) at equilibrium, respectively; K_L (L/g) is the Langmuir constant; and Q_m (g/mg) is the maximum adsorption capacity for monolayer formation on the adsorbent. The linear form of the Langmuir isotherm, represented by eq. (6), was used to determine the K_L and Q_m values from the linear and angular coefficients obtained by

$$\frac{C_e}{Q_e} = \frac{1}{K_L Q_m} + \frac{C_e}{Q_m} \tag{6}$$

The Q_m values calculated for CCTSL according to Langmuir isotherm model are given in Table VI. The linearizations according to the Langmuir model of adsorption isotherm for various metal(II) ions by CCTSL (Fig. 10) showed good R values (>0.99) with the experimental data from the adsorption equilibrium of metal ions, which homogeneous adsorption, which meant a monolayer.[36]

The nature and number of coordination sites present in the chitosan polymer influences the adsorption capacity of chitosan derivative.[37] From this study, we also inferred that the crosslinking of chitosan with a polydentate crosslinker containing nitrogen and hydroxyl donors showed higher adsorption capacities than other crosslinkers, which did not have coordinating sites.

CONCLUSIONS

A new CCTSL was synthesized and characterized. The adsorption capacities of this derivative toward various metal ions were higher than the free chitosan and were comparable to that of other CCTSLs reported in the literature. The higher adsorption capacity toward Cu^{2+} ion than the other metal ions studied indicated that it showed selectivity toward Cu^{2+} ions in aqueous solution, and hence, it could be used to extract Cu^{2+} ions from industrial wastewater.

References

1. Hu, Y.; Wu, Y.; Cai, J.; Ma, Y.; Wang, B.; Xia, K.; He, X. Int J Mol Sci 2007, 8, 1.
2. Prabaharan, M. J Biomater Appl 2008, 23, 5.
3. Cai, Z. S.; Song, Z. Q.; Yang, C. S.; Shang, S. B.; Yin, Y. B. J Appl Polym Sci 2009, 111, 3010.
4. Oshita, K.; Noguchi, O.; Oshima, M.; Motomizu, S. Anal Sci 2007, 23, 1203.
5. Chew, J. L.; Wolfowicz, C. B.; Mao, H. Q.; Leong, K. W.; Chua, K. Y. Vaccine 2003, 21, 2720.
6. Chen, X. G.; Lee, C. M.; Park, H. J. J Agric Food Chem 2003, 51, 3135.
7. Qu, R.; Sun, C.; Ji, C.; Wang, C.; Chen, H.; Niu, Y.; Liang, C.; Song, Q. Carbohydr Res 2008, 343, 267.
8. Chen, A. H.; Liu, S. C.; Chen, C. Y. J Hazard Mater 2008, 154, 184.
9. Shimizu, Y.; Nakamura, S.; Saito, Y.; Nakamura, T. J Appl Polym Sci 2008, 107, 1578.
10. Hao, X.; Chang, Q.; Li, X. J Appl Polym Sci 2009, 112, 135.
11. Ding, P.; Huang, K. L.; Li, G. Y.; Zeng, W. W. J Hazard Mater 2007, 146, 58.
12. Rodrigues, C. A.; Laranjeira, M. C. M.; Favere, V. T.; Stadler, E. Polymer 1998, 39, 5121.
13. Webster, A.; Halling, M. D.; Grant, D. M. Carbohydr Res 2007, 342, 1189.
14. Schwarzenbach, G.; Flaschka, H. Complexometric Titrations; Methuen: London, 1969; p 256.
15. Sheldrick, G. M. SHELX 97: Programs for the Refinement of Crystal Structures; University of Göttingen: Göttingen, Germany, 1997.
16. Yi, Y.; Wang, Y.; Ye, F. Colloids Surf A 2006, 277, 69.
17. Wan, M.-W.; Petrisor, I. G.; Lai, H.-T.; Kim, D.; Yen, T. F. Carbohydr Polym 2004, 55, 249.
18. Justi, K. C.; Laranjeira, M. C. M.; Neves, A.; Mangrich, A. S.; Fávere, V. T. Polymer 2004, 45, 6285.
19. Yang, Z.; Cheng, S. J Appl Polym Sci 2003, 89, 921.
20. Silverstein, R. M.; Bassler, G. C.; Morill, T. C. Spectrometric Identification of Organic Compounds, 5th ed.; Wiley: New York, 1991; Chapter 3.
21. Demetgül, C.; Serin, S. Carbohydr Polym 2008, 72, 506.
22. Sun, S.; Wang, A. J Hazard Mater B 2006, 131, 03.
23. Guinesi, L. S.; Cavalheiro, E. T. G. Carbohydr Polym 2006, 65, 557.
24. Pikus, T. J.; Charmas, W.; Gawdzik, B. J Appl Polym Sci 2000, 75, 142.
25. Krishnapriya, K. R.; Kandaswamy, M. Anal Sci 2008, 24, 1045.
26. Inukai, Y.; Chinen, T.; Matsuda, T.; Kaida, Y.; Yasuda, S. Anal Chim Acta 1998, 371, 187.
27. Sun, S.; Wang, A. Sep Purif Technol 2006, 49, 197.
28. Inoue, K.; Baba, Y.; Yoshizuka, K. Bull Chem Soc 1993, 66, 2915.
29. Yang, Z.; Shu, J.; Zhang, L.; Wang, Y. J Appl Polym Sci 2006, 100, 3018.
30. Hwang Chen, A.; Chang Liu, S.; Chen, C.-Y. J Hazard Mater 2008, 154, 184.
31. Ngah, W. S. W.; Endud, C. S.; Mayanar, R. React Funct Polym 2002, 50, 181.
32. Hirayama, N.; Ichitani, N.; Kubono, K.; Matsuoka, Y.; Kokusen, H.; Honjo, T. Talanta 1997, 44, 2019.
33. Baba, Y.; Aoya, Y.; Ohe, K.; Nakamura, S.; Oshima, T. J Chem Eng Jpn 2005, 38, 887.
34. Hernández, R. B.; Yolac, O. R.; Ramalho Mercê, A. L. J Braz Chem Soc 2007, 18, 1388.
35. Cestari, A. R.; Vieira, E. F. S.; Matos, J. D. S.; Dos Anjos, D. S. C. J Chem Thermodyn 2005, 285, 288.
36. Justi, K. C.; Fávere, V. T.; Laranjeira, M. C. M.; Neves, A.; Peralta, R. A. J Colloid Interface Sci 2005, 291, 369.
37. Cestari, A. R.; Vieira, E. F. S.; Mattos, C. R. S. J Chem Thermodyn 2006, 38, 1092.